PERMAFROST AND PERIGLACIAL PROCESSES
Permafrost and Periglac. Process. **27**: 377–389 (2016)
Published online 8 August 2016 in Wiley Online Library
(wileyonlinelibrary.com) DOI: 10.1002/ppp.1912

Recent Advances (2008–2015) in the Study of Ground Ice and Cryostratigraphy

Graham L. Gilbert,[1,2]* *Mikhail Kanevskiy*[3] *and Julian B. Murton*[4]

[1] Department of Arctic Geology, The University Centre in Svalbard, Longyearbyen, Norway
[2] Department of Earth Science, The University of Bergen, Bergen, Norway
[3] Institute of Northern Engineering, University of Alaska Fairbanks, Fairbanks, AK, USA
[4] Permafrost Laboratory, Department of Geography, University of Sussex, Brighton, UK

ABSTRACT

Cryostratigraphy involves the description, interpretation and correlation of ground-ice structures (cryostructures) and their relationship to the host deposits. Recent advances in the study of ground ice and cryostratigraphy concern permafrost aggradation and degradation, massive-ice formation and evaluation of ground-ice content. Field studies have increased our knowledge of cryostructures and massive ground ice in epigenetic and syngenetic permafrost. Epigenetic permafrost deposits are relatively ice-poor and composed primarily of pore-filled cryostructures, apart from an ice-enriched upper section and intermediate layer. Syngenetic permafrost deposits are commonly identified from cryostructures indicative of an aggrading permafrost table and are characterised by a high ice content, ice-rich cryofacies and nested wedge ice. Degradation of ice-rich permafrost can be marked by thaw unconformities, truncated buried ice wedges, ice-wedge pseudomorphs and organic-rich 'forest beds'. Studies of massive ground ice have focused on wedge ice, thermokarst-cave ice, intrusive ice and buried ice. Significant advances have been made in methods for differentiating between tabular massive-ice bodies of glacier and intrasedimental origin. Recent studies have utilised palynology, isotope geochemistry and hydrochemistry, in addition to sedimentary and cryostratigraphic analyses. The application of remote sensing techniques and laboratory methods such as computed tomography scanning has improved estimations of the ice content of frozen sediments. Copyright © 2016 John Wiley & Sons, Ltd.

KEY WORDS: cryostratigraphy; ground ice; permafrost; cryostructures

INTRODUCTION

Cryostratigraphy concerns the distribution and organisation of ground ice in soil, sediment or bedrock. It can be defined as 'the study of layering within permafrost; based on the description and interpretation of ice, sediment and rock, cryostratigraphy identifies and correlates stratigraphic units – usually layers – of permafrost' (Murton, 2013, p. 174). The value of cryostratigraphy stems from the fact that ground ice within sediment produces structures whose identification can elucidate the thermal history and origin of the substrate, because ground-ice formation, morphology and preservation are influenced by various climatic, geologic and environmental factors (Katasonov, 2009; French and Shur, 2010; Popov, 2013; Murton, 2013). Ground ice may be preserved indefinitely in permafrost environments, providing an enduring palaeoenvironmental archive. The principles of cryostratigraphy and general problems related to ground-ice studies have been recently discussed in English (French and Shur, 2010; Y.K. Vasil'chuk, 2012; Murton, 2013) and in Russian (Rogov, 2009; Badu, 2010; Shpolyanskaya, 2015).

Ice-rich permafrost is commonly associated with frost-susceptible sediment and occurs where moisture is sufficient for ground-ice formation or where ice is buried (Murton, 2013). Conditions conducive to extensive ground-ice formation have existed for much of the Quaternary Period in Arctic and Subarctic lowlands underlain by fine-grained sediments. Hence, the geographical distribution of recent cryostratigraphic studies has focused mainly on northern and central Siberia, Alaska and western Arctic Canada (Figure 1).

This review identifies recent advances in the understanding of ground ice and cryostratigraphy of present-day permafrost regions based on literature published between 2008 and 2015. We focus on four cryostratigraphic themes:

* Correspondence to: *Graham L. Gilbert*, Department of Arctic Geology, The University Centre in Svalbard, Longyearbyen, Norway. E-mail: Graham.Gilbert@unis.no

Received 21 January 2016
Revised 5 May 2016
Accepted 17 June 2016

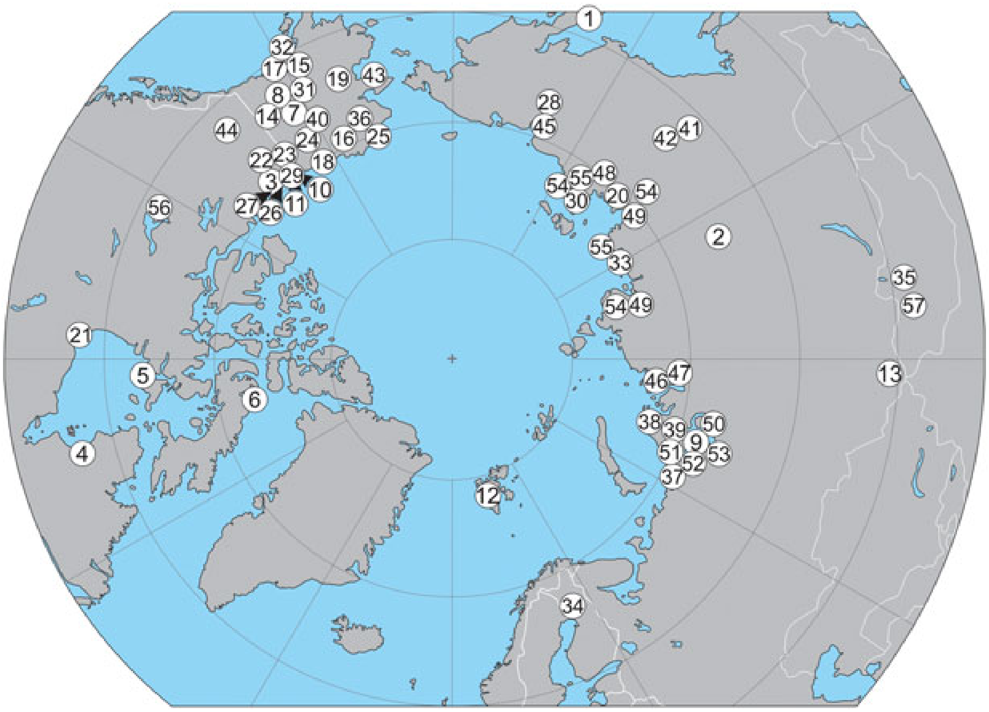

Figure 1 Approximate locations of field investigations included in this review. Regional studies and investigations which predate 2008 are not included. (1) Abramov *et al*. (2008); (2) Alexeev *et al*. (2016); (3) Bode *et al*. (2008); (4) Calmels *et al*. (2008); (5) Calmels *et al*. (2012); (6) Coulombe *et al*. (2015); (7) Douglas *et al*. (2011); (8) Fortier *et al*. (2012); (9) Fotiev (2014); (10) Fritz *et al*. (2011); (11) Fritz *et al*. (2012); (12) Härtel *et al*. (2012); (13) Iwahana *et al*. (2012); (14) Kanevskiy *et al*. (2008); (15) Kanevskiy *et al*. (2011); (16) Kanevskiy *et al*. (2012); (17) Kanevskiy *et al*. (2013a); (18) Kanevskiy *et al*. (2013b); (19) Kanevskiy *et al*. (2014); (20) Katasonov (2009); (21) Kuhry (2008); (22) D. Lacelle *et al*. (2009); (23) Lauriol *et al*. (2010); (24) Meyer *et al*. (2008); (25) Meyer *et al*. (2010); (26) Morse and Burn (2013); (27) Murton (2009); (28) Murton *et al*. (2015); (29) O'Neill and Burn (2012); (30) Opel *et al*. (2011); (31) Osterkamp *et al*. (2009); (32) Riddle and Rooney (2012); (33) Schirrmeister *et al*. (2011); (34) Seppälä (2011); (35) Sharkuu *et al*. (2012); (36) Shur *et al*. (2012); (37) Slagoda *et al*. (2010); (38) Slagoda *et al*. (2012a); (39) Slagoda *et al*. (2012b); (40) Sliger *et al*. (2015); (41) Spektor *et al*. (2011); (42) Spektor *et al*. (2008); (43) Stephani *et al*. (2012); (44) Stephani *et al*. (2014); (45) Strauss *et al*. (2012); (46) Streletskaya and Vasilev (2012); (47) Streletskaya *et al*. (2011); (48) Tumskoy (2012); (49) Ulrich *et al*. (2014); (50) Y. K. Vasil'chuk *et al*. (2014); (51) Y. K. Vasil'chuk *et al*. (2009); (52) Y. K. Vasil'chuk *et al*. (2011); (53) Y. K. Vasil'chuk *et al*. (2012); (54) Wetterich *et al*. (2011); (55) Wetterich *et al*. (2014); (56) Wolfe *et al*. (2014); and (57) Yoshikawa *et al*. (2013).

(1) permafrost aggradation; (2) renewed aggradation of permafrost following degradation; (3) massive ground ice; and (4) evaluation of ground-ice content. The dating of permafrost and the cryostratigraphy of past permafrost regions (e.g. northwest Europe) are beyond the scope of this review.

PERMAFROST AGGRADATION

Cryostratigraphic reconstructions of permafrost aggradation tend to focus on ground-ice development in unconsolidated sediments and classify permafrost in terms of its time of formation relative to the deposition of the host material. *Epigenetic permafrost* aggrades after the host material has formed, sometimes with a time lag of thousands or millions of years (French and Shur, 2010). *Syngenetic permafrost* aggrades at a rate proportional to the sedimentation rate at the ground surface, and characterises cold-climate landscapes influenced by relatively continuous deposition by fluvial, colluvial, lacustrine or aeolian processes. *Quasi-syngenetic permafrost* forms the top layer of permafrost (ice-rich intermediate layer) by upwards freezing as a result of the gradual thinning of the active layer over time – usually due to the development of surface vegetation (Shur, 1988). Many permafrost bodies consist of epigenetic, syngenetic and/or quasi-syngenetic components and so are *polygenetic*. The distinction between them is made by systematically analysing the spatial distribution of cryostructures and the nature of ground ice.

Cryostructures, or patterns formed by ice inclusions in frozen ground, are defined as structures that reflect the amount and distribution of pore and segregated ice within frozen sediment (French and Shur, 2010). Individual cryostructures are identified based on the shape, distribution and proportions of ice, sediment or rock within frozen ground (Murton, 2013). Nine cryostructures are commonly described in recent literature (Figure 2). *Pore* cryostructure develops where porewater freezes *in situ* in the interstices between mineral grains, forming an ice cement; the pore cryostructure may be visible to the naked eye in sands and gravels or non-visible in silts or clays (Figure 2A). *Organic-matrix* cryostructure forms where ice fills void spaces in organic material (e.g. peat or organic-rich soil) (Figure 2B). *Crustal* cryostructure occurs where ice segregation creates an ice crust around an object such as a rock

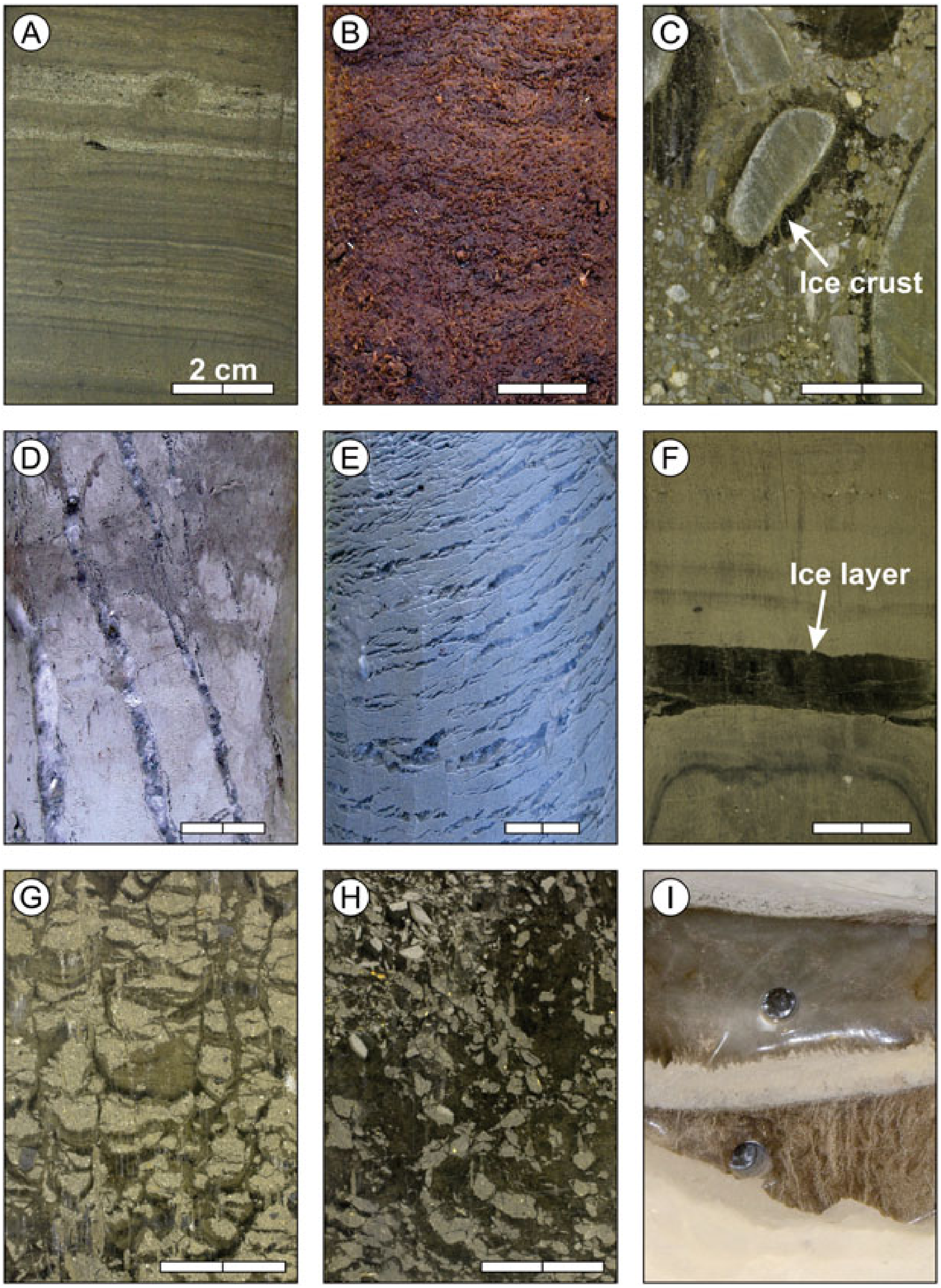

Figure 2 Simplified classification of cryostructures in unconsolidated sediments based on a classification presented by Murton (2013), which is modified from previous classifications. All photographs are oriented vertically such that the long axis of the image is perpendicular to the ground surface. (A) Pore cryostructure – note the absence of visible ice. (B) Organic-matrix cryostructure – ice present in the void space but not visible. (C) Crustal cryostructure. (D) Vein cryostructure. (E) Lenticular cryostructure. (F) Layered cryostructure. (G) Reticulate cryostructure. (H) Ataxitic cryostructure. (I) Solid cryostructure – thermokarst-cave (pool) ice overlying a vertically foliated ice wedge. Two drill holes several centimetres in diameter are visible in the ice.

clast or wood fragment in frost-susceptible material (Figure 2C). *Vein* cryostructure denotes ice veins that are inclined to vertical in orientation (Figure 2D). *Lenticular* cryostructure denotes lens-shaped ice bodies, often horizontal to subhorizontal, formed by ice segregation in frost-susceptible material (Figure 2E). *Layered* (or bedded) cryostructure comprises horizontal to dipping ice layers formed by ice segregation or injection of pressurised water (Figure 2F). *Reticulate* cryostructure represents a three-dimensional (3D) network of vertical ice veins and horizontal ice lenses that separate clayey or silty sediment blocks (Figure 2G). *Ataxitic* (suspended) cryostructure develops where sediment grains or aggregates are suspended in ice; in many cases, it forms in the intermediate layer at the top of permafrost (Figure 2H). *Solid* cryostructure occurs where bodies of ice exceed 10 cm in thickness (Figure 2I). These cryostructures are useful for logging of permafrost sequences, but in reality some cryostructures are transitional, composite or hierarchical in nature (Murton, 2013).

The development of cryostructures relates to three main factors: (1) the physical properties of soil, sediment or bedrock; (2) moisture availability; and (3) the mode of permafrost formation (epigenetic, syngenetic or quasi-syngenetic). A key property is the grain size distribution (particularly the proportion of silt) and packing of grains, which influence the frost susceptibility of the host sediment (i.e. the degree to which the soil favours the formation of segregated ice). Frost susceptibility in soils depends primarily on the continuous network of unfrozen water films in the frozen fringe. Moister sites promote the formation of ice-rich cryostructures compared to drier ones (Murton, 2013; Stephani *et al*., 2014).

Distinguishing cryostructures is scale-dependent and may be difficult when working with cores. The small diameter of cores (mostly between 5 cm and 10 cm) means that lateral continuity of ground-ice bodies in many cases cannot be established. For instance, it may not be possible to distinguish between lenticular and layered cryostructures at the core scale. Natural sections or trial pits best reveal cryostructures.

Epigenetic Permafrost

When the ground surface begins to experience cold subaerial conditions, epigenetic permafrost aggrades downward. Under such conditions, ground ice and permafrost decrease in age with depth.

Outside of areas with buried ice, epigenetic permafrost tends to be ice-poor, with wedge and segregated ice concentrated mostly in the top few metres. However, ice-rich epigenetic permafrost (including massive-ice bodies of segregated or intrusive origin) may form at any depth where the freezing front encounters a significant source of groundwater. The distance between visible ice lenses generally increases with depth, whereas the overall ice content decreases. The ice-rich top, in many cases, may be explained by the formation of the ice-rich intermediate layer, which results from a gradual decrease in active-layer thickness (mostly due to the accumulation of organic matter) and is characterised by an ataxitic (suspended) cryostructure (French and Shur, 2010). Formation of the intermediate layer is considered ‘quasi-syngenetic’ because permafrost aggrades upward without any sedimentation on the ground surface (Shur *et al*., 2011).

Cryostructures of ataxitic, lenticular and layered type are common in the intermediate layer (Osterkamp *et al*., 2009; Calmels *et al*., 2012). The type of cryostructure in this layer depends strongly on the rate of upward permafrost aggradation. Prolonged stability of the permafrost table favours layered cryostructures (so-called ‘ice belts’, discussed below), whereas slow aggradation of the permafrost table favours ataxitic cryostructures (Calmels *et al*., 2012), as illustrated from till deposits in Yukon, Canada (Stephani *et al*., 2014).

Where the groundwater supply is limited, epigenetic freezing forms a pore cryostructure with very low ice content (Stephani *et al*., 2014), whose presence in frost-susceptible material is a hallmark of epigenetic permafrost. Reticulate cryostructures also indicate epigenetic permafrost, and are believed to develop by desiccation and shrinkage during sediment freezing while moisture migrates towards an advancing freezing front (French and Shur, 2010).

Ice-rich epigenetic permafrost commonly forms in sediments where groundwater is abundant. Layered and reticulate cryostructures characterise epigenetically frozen lacustrine silts in the lowlands of west-central Alaska, with the volume of visible segregated ice varying from 10 to 50 per cent, and ice lenses up to 10 cm thick (Kanevskiy *et al*., 2014). Similar cryostructures have been described in Nunavik, Canada (Calmels and Allard, 2008). Ice-rich epigenetic permafrost was also detected near Anchorage, close to the southern boundary of permafrost in Alaska (Riddle and Rooney, 2012). In the 10 m thick section of glaciolacustrine deposits (silty clay with numerous layers of segregated ice up to 70 cm thick) there, the average volume of visible ice exceeded 40 per cent (Kanevskiy *et al*., 2013a).

In the discontinuous permafrost zone, epigenetic permafrost often starts to form with the development of palsas or lithalsas, which may eventually transform into permafrost plateaus elevated above the initial ground surface by the accumulation of segregated ice. Palsas and lithalsas have been recently studied in Fennoscandia (Seppälä, 2011), the Altai and Sayan regions of Russia (Iwahana *et al*., 2012; Y. K. Vasil’chuk *et al*., 2015), the Northwest Territories (e.g. Wolfe *et al*., 2014) and northern Quebec, Canada (Kuhry, 2008; Calmels and Allard, 2008; Calmels *et al*., 2008), the Himalayas (Wünnemann *et al*., 2008) and Mongolia (Sharkuu *et al*., 2012).

Ice-rich syngenetic permafrost sometimes degrades, drains and subsequently re-establishes as epigenetic permafrost. Thawed and refrozen soils typically undergo a reduction in ice content when compared with their former state. However, in many cases, ice-rich quasi-syngenetic permafrost forms on top of such refrozen soils, usually due to the development of surface vegetation and formation of an organic-rich surface horizon (Stephani *et al*., 2014; Kanevskiy *et al*., 2014).

Bedrock hosts epigenetic permafrost in many areas, especially alpine settings and areas eroded by Pleistocene glaciers, for example, the Canadian Shield. Classification of cryostructures in bedrock adopted from the Russian permafrost literature (translated by Mel'nikov and Spesivtsev, 2000) is presented by French and Shur (2010). Pore and layered cryostructures in basalt lava have recently been described from Kamchatka (Abramov *et al*., 2008) and intrusive ice layers and lenses in limestones, dolomites, marls and kimberlites from central Yakutia (Alexeev *et al*., 2016).

Syngenetic Permafrost

Ground ice in syngenetic permafrost forms within aggrading sedimentary sequences during or soon after deposition, mainly as segregated ice at the top of permafrost (also named *aggradational ice*; Mackay, 1972; Cheng, 1983) or as syngenetic wedge ice. Layered and lenticular cryostructures record the progressively aggrading ground surface, and are typical of syngenetic permafrost (French and Shur, 2010). Russian studies of the 1950–60s (Katasonov, 2009; Popov, 2013) revealed rhythmic structure of syngenetic permafrost, formed by relatively uniform layers with a predominantly lenticular cryostructure separated by '*ice belts*' (distinct icy layers several millimetres to several centimetres thick that indicate the position of the permafrost table during periods when it was relatively stable). Cryostructures between ice belts have been termed '*microcryostructures*' (Kanevskiy *et al*., 2011), formed mainly by thin (<1 mm) densely spaced ice lenses and include microlenticular, microbraided and microataxitic types.

Moisture availability, soil texture and sedimentation rate strongly control cryostructure distribution in syngenetic permafrost. Two cryofacies diagnostic of syngenetic permafrost have been distinguished in organic-rich silts, in Yukon, Canada (Stephani *et al*., 2014). Microlenticular cryostructures formed in near-surface permafrost during periods of relatively rapid surface aggradation (e.g. by deposition of windblown silt). Conversely, ataxitic and reticulate cryostructures with thick ice belts formed during periods of slower siliciclastic sedimentation that favoured the accumulation of peat and resulted in active-layer thinning and formation of the intermediate layer. Buried ice-rich intermediate layers with thick ice belts and predominantly ataxitic cryostructure are typical of thick sequences of syngenetic permafrost (Stephani *et al*., 2014; Kanevskiy *et al*., 2011).

Syngenetic permafrost of Holocene age tends to be thinner than that of Pleistocene age. Currently, syngenetic permafrost forms in mineral soils within floodplains of Arctic rivers (Shur and Jorgenson, 1998), deltas (Morse and Burn, 2013) and areas of loess accumulation (Härtel *et al*., 2012), and the reported thickness of modern syngenetic permafrost seldom exceeds 5 m. Cryostratigraphic studies of syngenetic permafrost, however, have focused mainly on Pleistocene '*yedoma*' (or 'Ice Complex'), which represents relic ice-rich syngenetic permafrost with large ice wedges that formed in Siberia and North America during the Late Pleistocene (Figure 3A; Schirrmeister *et al*., 2013; Murton *et al*., 2015). Continued supply of fine-grained sediment favoured yedoma development over tens of thousands of years, producing syngenetic permafrost sequences often several tens of metres thick that archive Late Pleistocene environmental history. General maps of yedoma distribution in Siberia were presented by Konishchev (2009, 2011) and Kanevskiy *et al*. (2011), with the latter authors including a preliminary map of yedoma distribution in Alaska. Detailed maps of Siberian yedoma (scale 1:1 000 000) have been developed by Grosse *et al*. (2013) from Russian Quaternary geological maps. Yedoma sections have been recently described from northern Yakutia (Schirrmeister *et al*., 2011; Tumskoy, 2012; Strauss *et al*., 2012; Wetterich *et al*., 2011, 2014), central Yakutia (Spektor *et al*., 2008), Taymyr (Streletskaya and Vasilev, 2012), northern Alaska (Kanevskiy *et al*., 2011), interior Alaska (Kanevskiy *et al*., 2008; Meyer *et al*., 2008), the Seward Peninsula (Shur *et al*., 2012; Stephani *et al*., 2012) and Yukon (Froese *et al*., 2009; Pumple *et al*., 2015; Sliger *et al*., 2015).

Ground ice is abundant and buried cryosols are present within many yedoma sequences. Ground ice observed at 14 locations along the coast of the Laptev and East Siberian seas was primarily wedge ice, 'net-like reticulated' cryostructures and ice bands (Schirrmeister *et al*., 2011). The ice wedges were identified as syngenetic on the basis of their large size and morphology. Ice bands (belts in the Russian literature) were interpreted to reflect stable surface conditions and active-layer thicknesses, leading to ice enrichment of the near-surface permafrost. Buried cryosols within the yedoma contained peat 'nests' and terrestrial plant leaves and woody debris. Schirrmeister *et al*. (2011) attributed these deposits to formation subaerially in polygonal terrain.

PERMAFROST DEGRADATION AND RE-AGGRADATION

The degradation of ice-rich permafrost (thermokarst) may produce distinctive features in the cryostratigraphic record that indicate the depth or mode of past thermokarst activity prior to re-aggradation of permafrost. This is well illustrated in two case studies from yedoma regions, which are particularly susceptible to thermokarst. The first identified cryostratigraphic evidence for shallow degradation of permafrost in non-glaciated Yukon and Alaska during the last interglaciation: (1) buried relic ice wedges whose tops were thaw truncated at the base of a palaeo-active layer; (2) ice-wedge pseudomorphs formed by complete melting of ice wedges; (3) wood-rich organic silt deposits ('forest beds') that represent forest vegetation reworked by thaw slumping or deposition in thermokarst ponds or depressions; and (4) lenticular and reticulate cryostructures interpreted as segregated ice at the top of permafrost and the bottom of the active layer (Reyes *et al*., 2010). This study inferred a depth of thaw on the order of metres during the last interglaciation, highlighting the resilience of ice-rich discontinuous permafrost over glacial-interglacial timescales. The second case

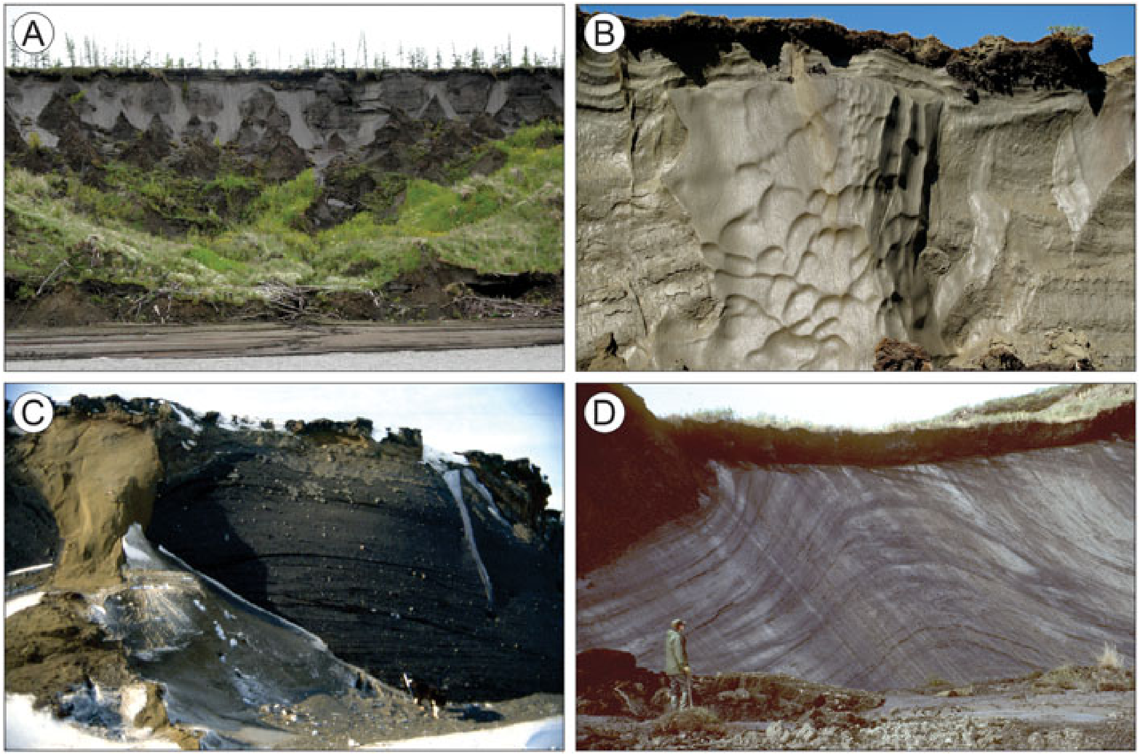

Figure 3 (A) Yedoma exposed in the headwall of a retrogressive thaw slump at Duvanny Yar, northeast Yakutia, Russia. Syngenetic ice wedges (lighter-coloured grey) enclose columns of silt (darker-coloured grey), some of which degrade to form conical thermokarst mounds (baydzherakhs). The top of the headwall is about 39 m above the level of the Kolyma River (in foreground). (B) Ice-rich *c*. 1 m thick intermediate layer with a thin active ice wedge on top of a large buried syngenetic ice wedge, 35 m high Itkillik River yedoma exposure, northern Alaska. (C) Buried basal ice from the Laurentide Ice Sheet, Mason Bay, Richards Island, Northwest Territories, Canada. Pebbles and cobbles protrude from the surface of massive ice, and folds occur within it. Sand wedge (left) and two ice wedges (right) penetrate massive ice. Dog and ice axe for scale (bottom centre). (D) Post-glacial intrasedimental massive ice at Peninsula Point, near Tuktoyaktuk, Northwest Territories, Canada. Anticline in banded massive ice underlies a small slump.

study used cryostratigraphic observations to evaluate the permafrost response to clearance of surface vegetation in discontinuous permafrost of the Klondike region, Yukon (Calmels *et al*., 2012). There, a thaw unconformity at a depth of about 2 m was interpreted to mark the thaw depth following deforestation during the gold rush era, beginning about 1900 AD.

MASSIVE GROUND ICE

Massive ice is a comprehensive term applied to large bodies of ground ice with ice contents exceeding 250 per cent by weight (van Everdingen, 1998). Recent studies of massive ice have focused on four main genetic classes (wedge ice, thermokarst-cave (pool) ice, intrusive ice and buried ice) and on the origin of tabular massive-ice bodies.

Wedge Ice

Ice wedges are the most common type of massive ice, and syngenetic wedges are particularly valuable in cryostratigraphy because both the wedge ice and surrounding sediments contain palaeoenvironmental archives. Syngenetic ice wedges grow both vertically and horizontally, resulting often in a vertically nested chevron pattern (Mackay, 1990). Syngenetic ice wedges in the outer Mackenzie Delta, Canada, have been identified from 'shoulders' indicative of vertical growth stages and from the cross-sectional width of the wedges decreasing towards the top of permafrost (Figure 3B; Morse and Burn, 2013). The ice wedges developed below a slowly aggrading surface.

A conceptual model of syngenetic ice-wedge development invokes micro-, meso- and macrocycles (Y.K. Vasil'chuk, 2013). Microcycles affect ice wedges by changes in active-layer depth and rates of deposition of thin sediment layers over timescales of several years to hundreds of years. Mesocycles of ice-wedge growth result from changes in water level, where ice wedges are located close to or under shallow water bodies. Deposits overlying wedge ice consist of alternating layers of peat (formed during exposure) and siliciclastic sediment (deposited during submergence). Ice-wedge growth is reduced or suspended during submergence. Macrocycles result from major changes in sedimentary regimes over timescales of tens of thousands to hundreds of thousands of years.

Syngenetic ice wedges account for a significant proportion of the ground-ice record in lowland permafrost environments, especially in yedoma. Recent studies of the isotopic or trapped gas composition in wedge ice have reconstructed palaeoclimate and investigated infilling processes (e.g. Meyer *et al*., 2010; Opel *et al*., 2011; Raffi and Stenni, 2011; Lachniet *et al*., 2012). For example, Streletskaya *et al*. (2011) identified a trend of warming palaeoclimate since the Late Weichselian from different generations of syngenetic ice wedges near the Kara Sea. St-Jean *et al*. (2011) showed that site-specific factors influence the infilling characteristics of wedge ice: in cold, dry settings, wedge ice shows evidence of snow densification, and in moister settings of freezing of liquid water.

Thermokarst-Cave Ice

Thermokarst-cave ice (or pool ice) forms by freezing of water trapped in underground cavities or channels (Murton, 2013), typically along degrading ice wedges (Figure 2I). Recent studies have described thermokarst-cave ice bodies underlain by silts with reticulate cryostructure in the CRREL permafrost tunnel, interior Alaska (Fortier *et al*., 2008; Kanevskiy *et al*., 2008; Douglas *et al*., 2011). Measurements performed along a 600 m long and 10 m high exposure at Barter Island (Alaskan Beaufort Sea coast) showed that numerous thermokarst-cave ice bodies occupied almost 2 per cent of the face of the coastal bluff (Kanevskiy *et al*., 2013b).

Intrusive Ice

Intrusive ice forms by freezing of water injected under pressure into freezing or frozen ground (Murton, 2013). Recent cryostratigraphic studies of intrusive ice have focused on stable isotope stratigraphy and the identification and development of tabular massive ice.

Stable isotope analysis has been applied to reconstruct the freezing processes and growth history of pingos. Two different isotopic patterns, indicative of open-system and semi-closed-system freezing, were observed in ice sections in an open-system (hydraulic) pingo in northwest Mongolia, indicating an oscillation between periods where the groundwater reservoir fed open-system ice lens development and those of flow interruption, forming a closed-system environment (Yoshikawa *et al*., 2013). Y. K. Vasil'chuk *et al*. (2014) distinguished between two periods of development in a closed-system (hydrostatic) pingo in northwest Siberia.

Massive bodies of intrusive ice may form following the drainage of palaeo-lake systems, or from the repeated injection of lake water into marine sediments following shoreline regression. In glaciolacustrine deposits of central Yukon, Lauriol *et al*. (2010) identified, using stable O and H isotopes and occluded gas composition, intrusive ice bodies (10 m wide and 3–4 m thick) that aggraded following the lowering of the water level in a palaeo-glacial lake. The glaciolacustrine sediments are underlain by permeable gravels and sands, which served as the water source during permafrost aggradation. The formation mechanism is therefore likely similar to growth conditions of hydrostatic pingos.

Buried Ice

Various types of ice bodies may be buried by soil or sediment. Recent literature on buried ice primarily concerns buried basal glacier ice (Murton, 2009; Fortier *et al*., 2012; Solomatin and Belova, 2012; Solomatin, 2013; Coulombe *et al*., 2015; Lacelle *et al*., 2015) and buried snow (Spektor *et al*., 2011). Investigations of cryostructures in basal ice from existing glaciers provide a basis for comparison with buried counterparts (e.g. Fortier *et al*., 2012).

Several stratigraphic characteristics aid in identifying buried glacier ice, including: (1) a discordant upper contact; (2) inclusions of glacial sediment (Figure 3C); and (3) dynamic metamorphic structures. A discordant upper contact is identified by the truncation of internal ice structures such as folds, stratification, and structural and textural heterogeneities (Solomatin and Belova, 2012). Such thaw or erosional unconformities develop due to either glaciofluvial erosion or the thaw front reaching the ice surface (Murton, 2013; Coulombe *et al*., 2015). Glaciotectonic deformation structures in ice-rich diamictons and ice structures similar to those in modern basal glacier ice may also serve as genetic indicators. Murton (2009) used an event stratigraphy related to the timing of glaciotectonic deformation to help distinguish between massive ice that was buried or at least glacially deformed from that which post-dated deformation and must be of intrasedimental origin. Though the stratigraphic context for massive ice may provide a good indication of the ice origin, it is not always conclusive, and interpretations may be strengthened by studies of ice crystallography, geochemistry and palynology.

Origin of Tabular Massive Ice

Most descriptions of tabular bodies of massive ice are from regions formerly occupied by Pleistocene glaciers or ice sheets. Such ice bodies commonly overlie coarse-grained (sand-rich) deposits, underlie fine-grained ones (muds) (Mackay and Dallimore, 1992) and contain sediment as individual particles or aggregates. Three models are generally employed to explain the origin of massive ice: (1) intrasedimental ice growth as segregated and/or intrusive ice; (2) burial of glacier ice; and (3) subglacial permafrost aggradation (Murton, 2013). Investigations commonly combine traditional stratigraphy and cryostratigraphy with other methods (ice crystallography, geochemistry and analysis of gas inclusions).

Recent studies of tabular massive ice have been conducted along the western Arctic coast of Canada (Murton, 2009; Fritz *et al*., 2011), central Yukon (Lauriol *et al*., 2010), the Alaskan Coastal Plain (Kanevskiy *et al*., 2013b), the Canadian Arctic islands (Coulombe *et al*., 2015) and northwest Siberia (Slagoda *et al*., 2010, 2012a, 2012b; Kritsuk, 2010; Leibman *et al*., 2011; Solomatin and Belova, 2012; Fotiev, 2014, 2015; Y. K. Vasil'chuk *et al.*, 2009, 2011, 2012, 2014; Vasiliev *et al.*, 2015). Intrasedimental and buried ice have been distinguished on several lines of evidence. This includes the stratigraphic, sedimentological and geomorphological setting of the ice bodies; the upper and lower contacts between the ice and the surrounding sediments; internal characteristics of the ice body (e.g. bubble characteristics, suspended sediment and deformation structures; Figure 3D); and ice palynology, stable isotope geochemistry and hydrochemistry. However, in many cases, the origin of tabular massive ice is disputed. For example, Y. K. Vasil'chuk (2012, p. 496) stated that 'It should be particularly noted that presently not a single massive ice body identified in the plain areas of the permafrost regions of Russia can be definitely identified as buried glacier ice.' In contrast, Solomatin and Belova (2012, p. 430) wrote in the same proceedings that 'The materials, experimental data, and theoretical concepts collected at the present time lead to the clear conclusion that tabular massive ice represents a single and separate genetic type of ground ice: the buried remnants of glaciers that formed during deglaciation of the ancient glaciation areas.'

Interpreting the origin of massive ice is often challenging because the growth of segregated ice, intrusive ice and gradations between them can occur in both non-glacial and subglacial settings. Intrasedimental bodies of tabular massive ice frequently display characteristics similar to those of buried glacier ice (Coulombe *et al.*, 2015). Recently, however, some valuable contributions have come from studies of ice palynology, isotope geochemistry and hydrochemistry. Studies in western Siberia have suggested that pollen and spores occur in most massive-ice bodies, and although redeposited pre-Quaternary palynomorphs of Cenozoic, Mesozoic and Palaeozoic age are common, the pollen of aquatic plants, horsetail spores, limnetic diatoms and green algae remains indicate a non-glacial genesis of the ice (A. C. Vasil'chuk and Y. K. Vasil'chuk, 2010, 2012). Vasiliev *et al.* (2015) reported extremely high concentrations of methane in tabular massive-ice bodies of the Yamal Peninsula, supporting the intrasedimental interpretation of tabular massive ice in this area.

Isotopic and hydrochemical analysis of massive ice is now commonly used to assist interpretation, with the values of and relations between $\delta^{18}O$, δD and d-excess providing insights into the processes of fractionation, sublimation and ionic segregation during freezing (D. Lacelle *et al.*, 2011; Michel, 2011), including in Martian regolith (D. Lacelle *et al.*, 2008). Such analyses often supplement field observations of the cryostratigraphy (Murton, 2009), and have permitted identification of buried perennial snowbank ice (D. Lacelle *et al.*, 2009), intrusive ice (Lauriol *et al.*, 2010) and aufeis (icing ice) (Lacelle and Vasil'chuk, 2013; Lacelle *et al.*, 2013) and basal regelation glacier ice (Fritz *et al.*, 2011, 2012).

A new classification of tabular massive ice, developed by Y. K. Vasil'chuk (2012), is based on three divisions. The first distinguishes between homogeneous and heterogeneous massive-ice bodies. *Homogeneous* massive-ice bodies have a similar genesis, composition and properties in all parts of a massive-ice complex. An example would be a single ice sill or body of massive segregated ice. *Heterogeneous* massive-ice bodies have a variable genesis, composition and properties across a massive-ice complex, and consist of two or more homogeneous ice bodies. Numerous examples occur on the Yamal Peninsula and adjacent regions of western Siberia (Y. K. Vasil'chuk *et al.*, 2009, 2011, 2012, 2014). The second division distinguishes between *autochthonous* (intrasedimental) and *allochthonous* (buried) ice, and the third division classifies the massive ice according to its specific genetic process (e.g. injection, segregation, infiltration, burial). Overall, this classification provides a valuable framework for investigating massive ice, and emphasises its genetic diversity.

GROUND-ICE CONTENT

Quantifying the amount and distribution of ground ice is necessary in order to predict permafrost landscape change in the future. Ground-ice content has become an important input to landscape and ecosystem models and in estimating organic carbon pools in permafrost (Kuhry *et al.*, 2013; Strauss *et al.*, 2013; Ulrich *et al.*, 2014). Cryostratigraphic observations provide valuable field data to help evaluate ground-ice content. Ground-ice content has recently been assessed using three distinct approaches: (1) landscape-scale estimation of wedge-ice volume (WIV) using remote sensing; (2) laboratory analysis of permafrost samples; and (3) fine-scale determination of ice volume by x-ray computed tomography (CT) scanning.

Y. K. Vasil'chuk (2009) reviewed different methods of WIV estimation (mainly based on ice-wedge geometry) developed by permafrost researchers since the 1960s. Several recent studies have estimated WIV in polygonal terrain using remotely sensed images (e.g. Bode *et al.*, 2008; Morse and Burn, 2013; Skurikhin *et al.*, 2013; Jorgenson *et al.*, 2015). Ulrich *et al.* (2014) presented a method for calculating WIV in yedoma and Holocene thermokarst basin deposits, utilising 3D surface models generated from satellite images to identify ice-wedge polygon morphometry. Individual wedge volume is estimated using measurements obtained from field data. Some assumptions are employed when calculating WIV: epigenetic ice wedges are usually assumed to have the shape of isosceles triangles or trapezoids in cross-section (Kanevskiy *et al.*, 2013b; Ulrich *et al.*, 2014), and syngenetic ice wedges that of a rectangular-shaped frontal cut (Strauss *et al.*, 2013). Ice-wedge size and morphology are commonly determined by field studies. Parameters determined from field measurements include the top and bottom width of individual wedges and the depth. Field data are used to parameterise 3D subsurface models and to upscale to the landscape scale.

The ice content of sediments containing pore, segregated or intrusive ice can be determined by laboratory analysis of permafrost samples. Gravimetric moisture content is commonly expressed on a dry basis (the ratio of the mass of ice in a sample to the mass of the dry sample). Phillips *et al*. (2015) compared dry- and wet-basis gravimetric moisture contents and concluded that the latter has some advantages when used for ice-rich mineral soils. Volumetric ice content (VIC) is the ratio of the volume of ice in a sample to the volume of the whole sample. Excess ice content is equal to the volume in excess of the pore volume in an unfrozen state, and estimations of excess ice content (e.g. O'Neill and Burn, 2012) correspond to thaw strain measurements commonly performed during geotechnical investigations (e.g. Kanevskiy *et al*., 2012). In ice-rich soils, excess ice content is similar to the volumetric content of visible ice. In ice-rich epigenetic permafrost, VIC can be estimated relatively easily by analysing photographs of frozen cores and exposures (Kanevskiy *et al*., 2013a, 2014). Total VIC of the upper layers of permafrost (which includes pore, segregated and massive ice) has been estimated based on a terrain-unit approach for the Beaufort Sea coastal area of Alaska (Kanevskiy *et al*., 2013b) and Yukon (Couture and Pollard, 2015).

CT scanning of frozen sediment cores provides a reasonable estimate of VIC and a non-destructive method of 3D imaging and analysing their internal structure (Calmels and Allard, 2008; Calmels *et al*., 2010, 2012; Lapalme *et al*., 2015). CT scans image features such as stratification, sediment properties, fractures, gas inclusions, ice distribution and density variations. The method utilises the density contrasts in the sample, allowing users to distinguish between gas, ice, organic and mineral components (Cnudde and Boone, 2013). Two limiting factors must be considered when determining VIC using image analysis of CT scans. Firstly, materials of similar densities are not easily differentiated. For example, organic-rich horizons (e.g. frozen, saturated peat) are similar in density to ice, which results in an overestimation of ice content unless the material can be correctly classified visually. Secondly, the spatial scan resolution (0.35 mm in the transverse direction and 0.5 mm in the longitudinal direction) limits the identification of pore ice in fine-grained sediment. Similarly, constituents (e.g. gas bubbles) that are smaller than the resolution size cannot be accounted for in volume calculations, which may lead to their underestimation, unless accounted for using calibration factors (Ducharme *et al*., 2015).

CONCLUSIONS AND PERSPECTIVES FOR FUTURE RESEARCH

Recent cryostratigraphic research in modern permafrost environments has focused on fine-grained deposits of aeolian, fluvial or lacustrine origin. As seen in Figure 1, however, relatively few cryostratigraphic studies have investigated permafrost in eastern Arctic Canada, Greenland and Scandinavia. Such landscapes include highly variable relief and depositional systems, where permafrost formation is closely tied to late Quaternary glacial and sea-level history. Evaluation of the cryostratigraphy of these environments may provide valuable insight into permafrost aggradation and ground-ice formation during the Holocene Epoch. Targeted studies in these locations may help to assess the nature of ground-ice formation in coarse-grained deposits, for example, in alluvial fans and colluvium.

Cryostructural classifications have been successfully applied to describe the occurrence and variability of ground ice in permafrost sediment sequences. To complement these largely descriptive and inferential studies, future research needs to investigate mechanistically the processes of cryostructure development. Freezing and thawing experiments under controlled field and laboratory conditions may allow hypothesis testing about cryostructure processes and boundary conditions, as well as quantification of rates of cryostructure formation.

The presence of ground ice has important consequences for landscape and infrastructure development as well as ecosystem and climate models. Recent studies into VIC have integrated a number of remotely sensed and indirect methods to assess ground-ice characteristics in permafrost. Future research needs to constrain the uncertainty in these estimations.

ACKNOWLEDGEMENTS

We would like to thank the two reviewers, D. Lacelle and one anonymous, and the Editor, C. R. Burn, for their constructive comments on the manuscript. M. Kanevskiy acknowledges the National Science Foundation (grants ARC 1023623 and ArcSEES 1233854) for financial support.

REFERENCES

Abramov A, Gruber S, Gilichinsky D. 2008. Mountain permafrost on active volcanoes: field data and statistical mapping, Klyuchevskaya volcano group, Kamchatka, Russia. *Permafrost and Periglacial Processes* **19**(3): 261–277. DOI:10.1002/ppp.622

Alexeev SV, Alexeeva LP, Kononov AM. 2016. Trace elements and rare earth elements in ground ice in kimberlites and sedimentary rocks of Western Yakutia. *Cold Regions Science and Technology* **123**: 140–148. DOI:10.1016/j.coldregions.2015.10.008

Badu YB. 2010. Cryolithology: Textbook. KDU: Moscow; 528 in Russian.

Bode JA, Moorman BJ, Stevens CW, Solomon SM. 2008. Estimation of ice wedge volume in the Big Lake Area, Mackenzie Delta, NWT, Canada. In Proceedings of the Ninth International Conference on Permafrost, Fairbanks, USA, 29 June–3 July 2008, Vol. **1**, Kane DL, Hinkel KM (eds). Institute for Northern Engineering, University of Alaska Fairbanks; 131–136.

Calmels F, Allard M. 2008. Segregated ice structures in various heaved permafrost landforms through CT scan. *Earth Surface Processes and Landforms* **33**: 209–225. DOI:10.1002/esp.1538

Calmels F, Allard M, Delisle G. 2008. Development and decay of a lithalsa in Northern Quebec: A geomorphological history. *Geomorphology* **97**: 287–299. DOI:10.1016/j.geomorph.2007.08.013

Calmels F, Clavano WE, Froese DG. 2010. Progress on x-ray computed tomography (CT) scanning in permafrost studies. In Proceedings Geo2010 Calgary–63rd Canadian Geotechnical Conference and 6th Canadian Permafrost Conference, 12–16 September 2010, Calgary, Canada; 1353–1358.

Calmels F, Froese DG, Clavano WR. 2012. Cryostratigraphic record of permafrost degradation and recovery following historic (1898-1992) surface disturbances in the Klondike region, central Yukon Territory. *Canadian Journal of Earth Sciences* **49**(8): 938–952. DOI:10.1139/e2012-023

Cheng G. 1983. The mechanism of repeated segregation for the formation of thick-layered ground ice. *Cold Regions Science and Technology* **8**: 57–66. DOI:10.1016/0165-232X(83)90017-4

Cnudde V, Boone MN. 2013. High-resolution x-ray computed tomography in geosciences: A review of the current technology and applications. *Earth-Science Reviews* **123**: 1–17. DOI:10.1016/j.earscirev.2013.04.003

Coulombe S, Fortier D, Shur Y, Kanevskiy M, Lacelle D. 2015. Cryofacies and cryostructures of massive ice found on Bylot Island, Nunavut. In Proceedings GeoQuébec 2015–68th Canadian Geotechnical Conference and 7th Canadian Permafrost Conference, 20–23 September 2015, Quebec, Canada.

Couture N, Pollard W. 2015. Ground ice determinations along the Yukon coast using a morphological model. In Proceedings GeoQuébec 2015–68th Canadian Geotechnical Conference and 7th Canadian Permafrost Conference, 20–23 September 2015, Quebec, Canada.

Douglas TA, Fortier D, Shur Y, Kanevskiy M, Guo L, Cai Y, Bray M. 2011. Biogeochemical and geocryological characteristics of wedge and thermokarst-cave ice in the CRREL permafrost tunnel, Alaska. *Permafrost and Periglacial Processes* **6**: 120–128. DOI:10.1002/ppp.709

Ducharme M-A, Allard M, Côté J, L'Hérault E. 2015. Measurements of permafrost thermal conductivity through CT-scan analysis. In Proceedings GeoQuébec 2015–68th Canadian Geotechnical Conference and 7th Canadian Permafrost Conference, 20–23 September 2015, Quebec, Canada.

Everdingen RO van. 1998revised May 2005. Multi-language Glossary of Permafrost and Related Ground-ice Terms. National Snow and Ice Data Center/World Data Center for Glaciology: Boulder, CO.

Fortier D, Kanevskiy M, Shur Y. 2008. Genesis of reticulate-chaotic cryostructure in permafrost. In Proceedings of the Ninth International Conference on Permafrost, June 29–July 3, 2008, Fairbanks, Alaska, Kane DL, Hinkel KM (eds), **1**. Institute of Northern Engineering, University of Alaska Fairbanks: Alaska; 451–456.

Fortier D, Kanevskiy M, Shur Y, Stephani E, Dillon M, Jorgenson T. 2012. Cryostructures of basal glacier ice as an object of permafrost study: observations from the Matanuska Glacier, Alaska. In Proceedings of the Tenth International Conference on Permafrost, June 25–29, 2012, Salekhard, Russia, Hinkel KM (ed), Vol. **1**. International contributions. The Northern Publisher: Salekhard, Russia; 107–112.

Fotiev SM. 2014. Massive ice beds, Marre-Sale Cape (western coast of the Yamal Peninsula). *Earth Cryosphere* **XVIII**(2): 34–46(in Russian).

Fotiev SM. 2015. Genesis and mechanism of formation of repeated-intrusive massive ice layers. *Earth Cryosphere* **XIX**(1): 27–36.

French H, Shur Y. 2010. The principles of cryostratigraphy. *Earth-Science Reviews* **101**: 190–206. DOI:10.1016/j.earscirev.2010.04.002

Fritz M, Wetterich S, Meyer H, Schirrmeister L, Lantuit H, Pollard WH. 2011. Origin and characteristics of massive ground ice on Herschel Island (western Canadian arctic) as revealed by stable water isotope and hydrochemical signatures. *Permafrost and Periglacial Processes* **22**(1): 26–38. DOI:10.1002/ppp.714

Fritz M, Wetterich S, Shirrmeister L, Meyer H, Lantuit H, Preusser F, Pollard WH. 2012. East Beringia and beyond: Late Wisconsinan and Holocene landscape dynamics along the Yukon Coastal Plain, Canada. *Palaeogeography, Palaeoclimatology, Palaeoecology* **319-320**: 28–45. DOI:10.1016/j.palaeo.2011.12.015

Froese DG, Zazula GD, Westgate JA, Preece SJ, Sanborn PT, Reyes AV, Pearce NJG. 2009. The Klondike goldfields and Pleistocene environments of Beringia. *GSA Today* **19**(8): 4–10. DOI:10.1130/GSATG54A.1

Grosse G, Robinson JE, Bryant R, Taylor MD, Harper W, DeMasi A, Kyker-Snowman E, Veremeeva A, Schirrmeister L, Harden J. 2013. Distribution of late Pleistocene ice-rich syngenetic permafrost of the Yedoma Suite in East and Central Siberia, Russia. USGS Geological Survey Open-File Report 2013-1078, 37pp.

Härtel S, Christiansen HH, Elberling B. 2012. Cryostratigraphy and ice content of the near-surface permafrost in lower Adventdalen, Svalbard. In Proceedings of the Tenth International Conference on Permafrost, June 25-29, 2012, Salekhard, Russia, Vol. **4** Extended abstracts. The Northern Publisher: Salekhard, Russia; 207–208.

Iwahana G, Fukui K, Mikhailov N, Ostanin O, Fujii Y. 2012. Structure of a Lithalsa in the Akkol Valley, Russian Altai Mountains. *Permafrost and Periglacial Processes* **23**(2): 107–118. DOI:10.1002/ppp.1734

Jorgenson T, Kanevskiy MZ, Shur Y, Moskalenko NG, Brown DRN, Wickland K, Striegl R, Koch J. 2015. Ground ice dynamics and ecological feedbacks control ice-wedge degradation and stabilization. *Journal of Geophysical Research: Earth Surface* **120**(11): 2280–2297. DOI:10.1002/2015JF003602

Kanevskiy M, Fortier D, Shur Y, Bray M, Jorgenson T. 2008. Detailed cryostratigraphic mapping of syngenetic permafrost in the Winze of the CRREL Permafrost Tunnel, Fox, Alaska. In *Proceedings of the Ninth International Conference on Permafrost, June 29 – July 3, 2008, Fairbanks, Alaska*, Kane DL, Hinkel KM (eds), Vol. **2**. Institute of Northern Engineering, University of Alaska Fairbanks; 889–894.

Kanevskiy M, Shur Y, Jorgenson MT, Stephani E. 2011. Cryostratigraphy of late Pleistocene syngenetic permafrost (yedoma) in northern Alaska, Itkillik River exposure. *Quaternary Research* **75**: 584–596. DOI:10.1016/j.yqres.2010.12.003

Kanevskiy M, Shur Y, Connor B, Dillon M, Stephani E, O'Donnell J. 2012. Study of the ice-rich syngenetic permafrost for road design (Interior Alaska). In Proceedings of the Tenth International Conference on Permafrost, June 25–29, 2012, Salekhard, Russia, Hinkel KM (ed), Vol. **1**. International contributions. The Northern Publisher: Salekhard, Russia; 191–196.

Kanevskiy M, Shur Y, Krzewinski T, Dillon M. 2013a. Structure and properties of ice-rich permafrost near Anchorage, Alaska. *Cold Regions Science and Technology* **93**: 1–11. DOI:10.1016/j.coldregions.2013.05.001

Kanevskiy M, Shur Y, Jorgenson MT, Ping C-L, Michaelson GJ, Fortier D, Stephani E, Dillon M, Tumskoy V. 2013b. Ground ice in the upper permafrost of the Beaufort Sea coast of Alaska. *Cold Regions Science and Technology* **85**: 56–70. DOI:10.1016/j.coldregions.2012.08.002

Kanevskiy M, Jorgenson MT, Shur Y, O'Donnell JA, Harden JW, Zhuang Q, Fortier D. 2014. Cryostratigraphy and permafrost evolution in the lacustrine lowlands of West-Central Alaska. *Permafrost and Periglacial Processes* **25**: 14–34. DOI:10.1002/ppp.1800

Katasonov EM. 2009. *Lithology of Frozen Quaternary Deposits* (*Cryolithology*) *of the*

Yana Coastal Plain (PhD thesis, Obruchev Permafrost Institute, 1954), Kaplina TN (ed). PNIIIS: Moscow; 176(in Russian).

Konishchev VN. 2009. Climate warming and permafrost. Moscow State University, Geography-Environment-Sustainability **1**: 4–19.

Konishchev VN. 2011. Permafrost response to climate warming. *Earth Cryosphere* **XV**(4): 13–16.

Kritsuk LN. 2010. Ground ice of West Siberia. Nauchniy Mir: Moscow; 352(in Russian).

Kuhry P. 2008. Palsa and peat plateau development in the Hudson Bay Lowlands, Canada: timing, pathways and causes. *Boreas* **37**(2): 316–327. DOI:10.1111/j.1502-3885.2007.00022.x

Kuhry P, Grosse G, Harden JW, Hughlius G, Koven CD, Ping C-L, Schirrmeister L, Tarnocai C. 2013. Characterization of the permafrost carbon pool. *Permafrost and Periglacial Processes* **24**: 146–155. DOI: 10.1002/ppp.1782

Lacelle D, Fisher DA, Clark ID, Berinstain A. 2008. Distinguishing between vapor- and liquid-formed ground ice in the northern martian regolith and potential for biosignatures preserved in ice bodies. *Icarus* **197**: 458–469. DOI:10.1016/j.icarus.2008.05.017

Lacelle D, St-Jean M, Lauriol B, Clark ID, Lewkowicz A, Froese DG, Kuehn SC, Zazula. 2009. Burial and preservation of a 30,000 year old perennial snowbank in Red Creek valley, Ogilvie Mountains, central Yukon, Canada. *Quaternary Science Reviews* **28**: 3401–3413. DOI:10.1016/j.quascirev.2009.09.013

Lacelle D, Davila AF, Pollard WH, Andersen D, Heldmann J, Marinova M, McKay CP. 2011. Stability of massive ground ice bodies in University Valley, McMurdo Dry Valleys of Antarctica: Using stable O–H isotope as tracers of sublimation in hyper-arid regions. *Earth and Planetary Science Letters* **301**: 403–411. DOI:10.1016/j.epsl.2010.11.028

Lacelle D, Lauriol B, Zazula G, Ghaleb B, Utting N, Clark ID. 2013. Timing of advance and basal conditions of the Laurentide Ice Sheet during the last glacial maximum in the Richardson Mountains, NWT. *Quaternary Research* **80**: 274–283. DOI:10.1016/j.yqres.2013.06.001

Lacelle D, Brooker A, Fraser RH, Kokelj SV. 2015. Distribution and growth of thaw slumps in the Richardson Mountains-Peel Plateau region, northwestern Canada. *Geomorphology* **235**: 40–51. DOI:10.1016/j.geomorph.2015.01.024

Lacelle DM, Vasil'chuk YK. 2013. Recent progress (2007-2012) in permafrost isotope geochemistry. *Permafrost and Periglacial Processes* **24**(2): 138–145. DOI:10.1002/ppp.1768

Lachniet MS, Lawson DE, Sloat AR. 2012. Revised ^{14}C dating of ice wedge growth in interior Alaska (USA) to MIS 2 reveals cold paleoclimate and carbon recycling in ancient permafrost terrain. *Quaternary Research* **78**: 217–225. DOI:10.1016/j.yqres.2012.05.007

Lapalme CM, Lacelle D, Davila AF, Pollard W, Fortier D, McKay CP. 2015. Cryostratigraphy of near-surface permafrost in University Valley, McMurdo Dry Valleys of Antarctica. In Proceedings GeoQuébec 2015–68 th Canadian Geotechnical Conference and 7th Canadian Permafrost Conference, 20–23 September 2015, Quebec, Canada.

Lauriol B, Lacelle D, St-Jean M, Clark ID, Zazula GD. 2010. Late Quaternary paleoenvironments and growth of intrusive ice in eastern Beringia (Eagle River valley, northern Yukon, Canada). *Canadian Journal of Earth Sciences* **47**: 941–955. DOI: 10.1139/E10-012

Leibman MO, Kizyakov AI, Lein AY, Perednya DD, Savvichev AS, Vanshtein BG. 2011. Sulfur and carbon isotopes within atmospheric, surface and ground water, snow and ice as indicators of the origin of tabular ground ice in the Russian Arctic. *Permafrost and Periglacial Processes* **22**(1): 39–48. DOI:10.1002/ppp.716

Mackay JR. 1972. The world of underground ice. *Annals of the American Association of Geographers* **62**: 1–22. DOI:10.1111/j.1467-8306.1972.tb00839.x

Mackay JR. 1990. Some observations on the growth and deformation of epigenetic, syngenetic and anti-syngenetic ice wedges. *Permafrost and Periglacial Processes* **1**: 15–29. DOI:10.1002/ppp.3430010104

Mackay JR, Dallimore SR. 1992. Massive ice in the Tuktoyaktuk area, western Arctic coast, Canada. *Canadian Journal of Earth Sciences* **29**(6): 1235–1249. DOI:10.1139/e92-099

Mel'nikov VP, Spesivtsev VI. 2000. Cryogenic Formations in the Earth's Lithosphere. Siberian Publishing Center UIGGM, Siberian Branch, Russian Academy of Sciences: Novosibirsk.

Meyer H, Yoshikawa K, Schirrmeister L, Andreev A. 2008. The Vault Creek Tunnel (Fairbanks Region, Alaska) – A Late Quaternary Palaeoenvironmental Permafrost Record. In Proceedings of the Ninth International Conference on Permafrost, June 29–July 3, 2008, Fairbanks, Alaska, Kane DL, Hinkel KM (eds), Vol. **2**. Institute of Northern Engineering, University of Alaska Fairbanks: Alaska; 1191–1196.

Meyer H, Schirrmeister L, Andreev A, Wagner D, Hubberten HW, Yoshikawa K, Bobrov A, Wetterich S, Opel T, Kandiano E, Brown J. 2010. Lateglacial and Holocene isotopic and environmental history of northern coastal Alaska – results from a buried ice-wedge system at Barrow. *Quaternary Science Reviews* **29**: 3720–3735. DOI:10.1016/j.quascirev.2010.08.005

Michel FA. 2011. Isotope characterisation of ground ice in northern Canada. *Permafrost and Periglacial Processes* **22**: 3–12. DOI: 10.1002/ppp.721

Morse PD, Burn CR. 2013. Field observations of syngenetic ice wedge polygons, outer Mackenzie Delta, western Arctic coast, Canada. *Journal of Geophysical Research: Earth Surface* **118**: 1320–1332. DOI:10.1002/jgrf.20086

Murton JB. 2009. Stratigraphy and palaeoenvironments of Richards Island and the eastern Beaufort Continental Shelf during the last glacial–interglacial cycle. *Permafrost and Periglacial Processes* **20**: 107–125. DOI:10.1002/ppp.647

Murton JB. 2013. Ground ice and cryostratigraphy. In Treatise on Geomorphology, Vol. 8, Glacial and Periglacial Geomorphology, Schoder JF, Giardino R, Harboor J (eds). Academic Press: San Diego; 173–201.

Murton JB, Goslar T, Edwards ME, Bateman MD, Danilov PP, Savvinov GN, Gubin SV, Ghaleb B, Haile J, Kanevskiy M, Lozhkin AV, Lupachev AV, Murton DK, Shur Y, Tikhonov A, Vasil'chuk AC, Vasil'chuk YK, Wolfe SA. 2015. Paleoenvironmental interpretation of yedoma silt (ice complex) deposition as cold-climate loess, Duvanny Yar, northeast Siberia. *Permafrost and Periglacial Processes* **26**: 208–288. DOI:10.1002/ppp.1843

O'Neill HB, Burn CR. 2012. Physical and temporal factors controlling the development of near-surface ground ice at Illisarvik, western Arctic coast, Canada. *Canadian Journal of Earth Sciences* **49**: 1096–1110. DOI:10.1139/E2012-043

Opel T, Dereviagin AY, Meyer H, Schirrmeister L, Wetterich S. 2011. Palaeoclimatic Information from Stable Water Isotopes of Holocene Ice Wedges on the Dmitrii Laptev Strait, Northeast Siberia, Russia. *Permafrost and Periglacial Processes* **22**(1): 84–100. DOI:10.1002/ppp.667

Osterkamp TE, Jorgenson MT, Schuur EAG, Shur YL, Kanevskiy MZ, Vogel JG, Tumskoy VE. 2009. Physical and ecological changes associated with warming permafrost and thermokarst in interior Alaska. *Permafrost and Periglacial Processes* **20**: 235–256. DOI:10.1002/ppp.656

Phillips M, Burn C, Wolfe S, Morse P, Gaanderse A, O'Neill B, Shugar D, Gruber S. 2015. Improving water content description of ice-rich permafrost soils. In Proceedings GeoQuébec 2015–68 th Canadian Geotechnical Conference and 7th Canadian Permafrost Conference, 20–23 September 2015, Quebec, Canada.

Popov AI. 2013. Selected works, and about him. Moscow: Nauchniy Mir; 536(in Russian).

Pumple J, Froese D, Calmels F. 2015. Characterizing permafrost valley fills along the Alaska Highway, southwest Yukon. In Proceedings GeoQuébec 2015–68th Canadian Geotechnical Conference and 7th Canadian Permafrost Conference, 20-23 September 2015, Quebec, Canada.

Raffi R, Stenni B. 2011. Isotopic composition and thermal regime of ice wedges in northern Victoria Land, East Antarctica. *Permafrost and Periglacial Processes* **22**(1): 65–83. DOI:10.1002/ppp.701

Reyes AV, Froese DG, Jensen BJL. 2010. Permafrost response to last interglacial warming: field evidence from non-glaciated Yukon and Alaska. *Quaternary Science Reviews* **29**: 3256–3274. DOI:10.1016/j.quascirev.2010.07.013

Riddle CH, Rooney JW. 2012. Encounters with relict permafrost in the Anchorage, Alaska, area. In *Proceedings of the Tenth International Conference on Permafrost, June 25–29, 2012, Salekhard, Russia*, Hinkel KM (ed), Vol. **1**. International contributions, The Northern Publisher: Salekhard, Russia; 323–328.

Rogov VV. 2009. Fundamentals of Cryogenesis. Novosibirsk: Geo; 203(in Russian).

Schirrmeister L, Kunitsky V, Grosse G, Wetterich S, Meyer H, Schwamborn G, Babiy O, Derevyagin A, Siegert C. 2011. Sedimentary characteristics and origin of the Late Pleistocene Ice Complex on north-east Siberian Arctic coastal lowlands and islands – A review. *Quaternary International* **241**: 3–25. DOI:10.1016/j.quaint.2010.04.004

Schirrmeister L, Froese D, Tumskoy V, Grosse G, Wetterich S. 2013. Yedoma: Late Pleistocene ice-rich syngenetic permafrost of Beringia. In Encyclopedia of Quaternary Science, Second edition, Elias SA, Mock CJ (eds), **2**. Elsevier: Amsterdam; 542–552.

Seppälä M. 2011. Synthesis of studies of palsa formation underlining the importance of local environmental and physical characteristics. *Quaternary Research* **75**: 366–370. DOI:10.1016/j.yqres.2010.09.007

Sharkuu N, Yoshikawa K, Anarmaa S. 2012. Perennial frost mounds in Mongolia. In Proceedings of the Tenth International Conference on Permafrost, June 25-29, 2012, Salekhard, Russia, Hinkel KM (ed), Vol. **1** International contributions. The Northern Publisher: Salekhard, Russia; 371–376.

Shpolyanskaya NA. 2015. Pleistocene-Holocene history of permafrost evolution in the Russian Arctic based on ground-ice studies. Institute of Computer Researches: Moscow-Izhevsk; 344(in Russian).

Shur YL. 1988. The upper horizon of permafrost soils. In *Proceedings of the Fifth International Conference on Permafrost*, Senneset K (ed), Vol. **1**. Tapir Publishers: Trondheim, Norway; 867–871.

Shur YL, Jorgenson MT. 1998. Cryostructure development on the floodplain of the Colville River Delta, northern Alaska. In *Permafrost, Proceedings of the 7th International Conference, Yellowknife, N.W.T., Canada*, Lewkowicz AG, Allard M (eds), Centre d'études Nordiques. Collection Nordicana 57, Université Laval: Quebec; 993–999.

Shur YL, Jorgenson MT, Kanevskiy MZ. 2011. Permafrost. In Encyclopedia of Earth Sciences Series, Encyclopedia of Snow, Ice and Glaciers, Singh VP, Singh P, Haritashya UK (eds). Springer: The Netherlands; 841–848 DOI: 10.1007/978-90-481-2642-2.

Shur YL, Kanevskiy M, Jorgenson T, Dillon M, Stephani E, Bray M. 2012. Permafrost degradation and thaw settlement under lakes in yedoma environment. In Proceedings of the Tenth International Conference on Permafrost, June 25-29, 2012, Salekhard, Russia, Hinkel KM (ed), **1** International contributions. The Northern Publisher: Salekhard, Russia; 383–388.

Skurikhin AN, Gangodagamage C, Rowland JC, Wilson CJ. 2013. Arctic tundra ice-wedge landscape characterization by active contours without edges and structural analysis using high-resolution satellite imagery. *Remote Sensing Letters* **4**: 1077–1086. DOI:10.1080/2150704X.2013.840404

Slagoda EA, Leibman MO, Opokina OL. 2010. Origin of deformations in Holocene-Quaternary deposits with tabular ground ice on Yugorsky peninsula. *Earth Cryosphere XIV* **4**: 30–41(in Russian).

Slagoda EA, Opokina OL, Kurchatova AN, Rogov VV. 2012a. Structure and composition of complex massive ice bodies in Late Pleistocene-Holocene sediments of the Marre-Sale Cape, West Yamal. In Proceedings of the Tenth International Conference on Permafrost, 25–29 June, 2012, Salekhard, Russia, Melnikov VP, Drozdov DD, Romanovsky VE (eds); 415–420.

Slagoda EA, Opokina OL, Rogov VV, Kurchatova AN. 2012b. Structure and genesis of the underground ice in the Neopleistocene-Holocene sediments of Marre-Sale cape, Western Yamal. *Earth Cryosphere XVI* **2**: 9–22(in Russian)..

Sliger M, Fortier D, deGrandpré I, Lapointe-Elmrabti L. 2015. Incidence of pleistocene-holocene climate on the concurrent landscape and permafrost development of the Beaver Creek region, southwest Yukon, Canada. In Proceedings GeoQuébec 2015– 68th Canadian Geotechnical Conference and 7th Canadian Permafrost Conference, 20-23 September 2015, Quebec, Canada.

Solomatin VI. 2013. Physics and geography of underground glaciation. Novosibirsk: Geo; 346(in Russian).

Solomatin VI, Belova NG. 2012. Proof of the glacier origin of tabular massive ice. In Proceedings of the Tenth International Conference on Permafrost, June 25-29, 2012, Salekhard, Russia, Melnikov VP, Drozdov DS, Romanovsky VE (eds), Vol. **2**. Translations of Russian contributions. The Northern Publisher: Salekhard, Russia; 427–432.

Spektor VB, Spektor VV, Bakulina NT. 2008. New data on the Ice Complex of the Lena-Amga rivers plain (Central Yakutia). In Proceedings of the Ninth International Conference on Permafrost, University of Alaska Fairbanks, Fairbanks, **2**; 1681–1684.

Spektor VB, Spektor VV, Bakulina NT. 2011. Buried Snow in the Lena-Amga Plain. *Earth Cryosphere* **15**(4): 16–21(in Russian).

Stephani E, Kanevskiy M, Dillon M, Bray M, Shur Y. 2012. Cryostratigraphy of Yedoma (Ice Complex) in Seward Peninsula, Alaska. In Tenth International Conference on Permafrost, June 25-29, 2012, Salekhard, Russia, Vol. **4**. Extended abstracts. Fort Dialog-Iset: Ekaterinburg, Russia; 569–570.

Stephani E, Fortier D, Shur Y, Fortier R, Doré G. 2014. A geosystems approach to permafrost investigations for engineering applications, an example from a road stabilization experiment, Beaver Creek, Yukon, Canada. *Cold Regions Science and Technology* **100**: 20–35. DOI:10.1016/j.coldregions.2013.12.006

St-Jean M, Lauriol B, Clark ID, Lacelle D, Zdanowicz C. 2011. Investigation of ice-wedge infilling processes using stable oxygen and hydrogen isotopes, crystallography and occluded gases (O_2, N_2, Ar). *Permafrost and Periglacial Processes* **22**: 49–64. DOI:10.1002/ppp.680

Strauss J, Schirrmeister L, Wetterich S, Borchers A, Davydov SP. 2012. Grain-size properties and organic-carbon stock of Yedoma Ice Complex permafrost from the Kolyma lowland, northeastern Siberia.

Global Biogeochemical Cycles **26**: GB3003. DOI:10.1029/2011GB00410410

Strauss J, Schirrmeister L, Grosse G, Wetterich S, Ulrich M, Herzschuh U, Hubberten H-W. 2013. The deep permafrost carbon pool of the Yedoma region in Siberia and Alaska. *Geophysical Research Letters* **40**(23): 6165–6170. DOI:10.1002/2013GL058088

Streletskaya I, Vasiliev A, Meyer H. 2011. Isotopic composition of syngenetic ice wedges and palaeoclimatic reconstruction, western Taymyr, Russian Arctic. *Permafrost and Periglacial Processes* **22**: 101–106. DOI:10.1002/ppp.707

Streletskaya ID, Vasilev AA. 2012. The ice complex of western Taymyr. In Proceedings of the Tenth International Conference on Permafrost, June 25-29, 2012, Salekhard, Russia, Melnikov VP, Drozdov DS, Romanovsky VE (eds), **2** Translations of Russian contributions. The Northern Publisher: Salekhard, Russia; 433–438.

Tumskoy VE. 2012. Peculiarities of cryolithogenesis in Northern Yakutia (middle Neopleistocene to Holocene). *Earth Cryosphere XVI* **1**: 2–21(in Russian).

Ulrich M, Grosse G, Strauss J, Schirrmeister L. 2014. Quantifying Wedge-Ice Volumes in Yedoma and Thermokarst Basin Deposits. *Permafrost and Periglacial Processes* **25**: 151–161. DOI:10.1002/ppp.1810

Vasil'chuk AC, Vasil'chuk YK. 2010. Local pollen spectra as a new criterion for nonglacial origin of massive ice. *Transactions* (*Doclady*) *of Russian Academy of Sciences*. *Earth Sciences* **433**: 985–990. DOI:10.1134/S1028334X10070305

Vasil'chuk AC, Vasil'chuk YK. 2012. Pollen and spores as massive ice origin indicators. In Proceedings of the Tenth International Conference on Permafrost, June 25-29, 2012, Salekhard, Russia, Melnikov VP, Drozdov DD, Romanovsky VE (eds), Vol. **2**. The Northern Publisher: Salekhard, Russia; 487–492.

Vasil'chuk YK. 2009. New approach to estimation of wedge-ice volume. *Inzhenernaya Geologiya (Engineering Geology)* **4**: 40–47(in Russian).

Vasil'chuk YK. 2012. Classification of Massive Ice. In Proceedings of the Tenth International Conference on Permafrost, June 25-29, 2012, Salekhard, Russia, Melnikov VP, Drozdov DD, Romanovsky VE (eds), Vol. **2**. The Northern Publisher: Salekhard, Russia; 493–497.

Vasil'chuk YK. 2013. Syngenetic ice wedges: Cyclical formation, radiocarbon age and stable isotope records by Yurij K. Vasil'chuk, Moscow University Press, Moscow, 2006, 404 pp, ISBN 5-211-05212-9 (Monograph Synopsis). *Permafrost and Periglacial Processes* **24**: 82–93. DOI:10.1002/ppp.1764

Vasil'chuk YK, Vasil'chuk AC, Budantseva NA, Chizhova JN, Papesch W, Podborny YY, Sulerzhitsky LD. 2009. Oxygen Isotope and Deuterium Indication of the Origin and ^{14}C Age of the Massive Ice, Bovanenkovo, Central Yamal Peninsula. *Doklady Earth Sciences* **429**: 1326–1332. DOI:10.1134/S1028334X09080194

Vasil'chuk YK, Budantseva NA, Vasil'chuk AC. 2011. Variations in $\delta^{18}O$, δD, and the concentration of pollen and spores in autochthonic heterogeneous massive ice on the Erkutayaha River in the southern part of the Yamal Peninsula. *Doklady Earth Sciences* **438**: 721–726. DOI:10.1134/S1028334X11050382

Vasil'chuk YK, Vasil'chuk AC, Budantseva NA. 2012. Isotopic and palynological compositions of a massive ice in the Mordyyakha River, Central Yamal Peninsula. *Doklady Earth Sciences* **446**: 1105–1109. DOI:10.1134/S1028334X12090164

Vasil'chuk YK, Budantseva NA, Vasilchuk AC, Yoshikawa K, Podborny YY, Chizhova JN. 2014. Isotope composition of pingo ice core in the Evoyakha river valley, North-West Siberia. *Earth Cryosphere* **XVIII**(4): 47–58(in Russian).

Vasil'chuk YK, Alexeev SV, Arzhannikov SG, Alexeeva LP, Budantseva NA, Chizhova JN, Arzhannikova AV, Vasil'chuk AC. 2015. Lithalsas in the Sentsa River Valley, Eastern Sayan Mountains, Southern Russia. *Permafrost and Periglacial Processes*In press DOI:10.1002/ppp.1876

Vasiliev AA, Streletskaya ID, Melnikov VP, Oblogov GE. 2015. Methane in ground ice and frozen Quaternary deposits of West Yamal. *Doklady Akademii Nauk [Transactions of Academy of Sciences] Earth Sciences* **465**(2): 1289–1292. DOI:10.1134/S1028334X15120168

Wetterich S, Rudaya N, Tumskoy V, Andreev AA, Opel T, Schirrmeister L, Meyer H. 2011. Last Glacial Maximum records in permafrost of the East Siberian Arctic. *Quaternary Science Reviews* **30**: 3139–3151. DOI:10.1016/j.quascirev.2011.07.020

Wetterich S, Tumskoy V, Rudaya N, Andreev AA, Opel T, Meyer H, Schirrmeister L, Hüls M. 2014. Ice Complex formation in arctic East Siberia during the MIS3 Interstadial. *Quaternary Science Reviews* **84**: 39–55. DOI:10.1016/j.quascirev.2013.11.009

Wolfe SA, Stevens CW, Gaanderse AJ, Oldenborger G. 2014. Lithalsa distribution, morphology and landscape associations in the Great Slave Lowland, Northwest Territories, Canada. *Geomorphology* **204**: 302–313. DOI:10.1016/j.geomorph.2013.08.014

Wünnemann B, Reinhardt C, Kotlia BS, Riedel F. 2008. Observations on the relationship between lake formation, permafrost activity and lithalsa development during the last 2000 years in the Tso Kar Basin, Ladakh, India. *Permafrost and Periglacial Processes* **19**: 341–358. DOI:10.1002/ppp.631

Yoshikawa K, Sharkhuu N, Sharkhuu A. 2013. Groundwater hydrology and stable isotope analysis of an open-system pingo in Northwestern Mongolia. *Permafrost and Periglacial Processes* **24**: 175–183. DOI:10.1002/ppp.1773